Characterization of a Germ-Line Deletion, Including the Entire *INK4/ARF* Locus, in a Melanoma-Neural System Tumor Family: Identification of *ANRIL*, an Antisense Noncoding RNA Whose Expression Coclusters with *ARF*

Eric Pasmant,[1] Ingrid Laurendeau,[1] Delphine Héron,[2] Michel Vidaud,[1] Dominique Vidaud,[1] and Ivan Bièche[1,3]

[1]Laboratoire de Génétique Moléculaire-Institut National de la Sante et de la Recherche Medicale U745, Faculté des Sciences Pharmaceutiques et Biologiques, Université Paris V; [2]Département de Génétique, Hôpital de la Pitié-Salpêtrière, Paris, France; and [3]Laboratoire d'Oncogénétique-Institut National de la Sante et de la Recherche Medicale U735, Centre René Huguenin, St-Cloud, France

Abstract

We have previously detected a large germ-line deletion, which included the entire *p15/CDKN2B-p16/CDKN2A-p14/ARF* gene cluster, in the largest melanoma-neural system tumor (NST) syndrome family known to date by means of heterozygosity mapping based on microsatellite markers. Here, we used gene dose mapping with sequence-tagged site real-time PCR to locate the deletion end points, which were then precisely characterized by means of long-range PCR and nucleotide sequencing. The deletion was exactly 403,231 bp long and included the entire *p15/CDKN2B, p16/CDKN2A*, and *p14/ARF* genes. We then developed a simple and rapid assay to detect the junction fragment and to serve as a direct predictive DNA test for this large French family. We identified a new large antisense noncoding RNA (named *ANRIL*) within the 403-kb germ-line deletion, with a first exon located in the promoter of the *p14/ARF* gene and overlapping the two exons of *p15/CDKN2B*. Expression of *ANRIL* mainly coclustered with *p14/ARF* both in physiologic (various normal human tissues) and in pathologic conditions (human breast tumors). This study points to the existence of a new gene within the *p15/CDKN2B-p16/CDKN2A-p14/ARF* locus putatively involved in melanoma-NST syndrome families and in melanoma-prone families with no identified *p16/CDKN2A* mutations as well as in somatic tumors. [Cancer Res 2007;67(8):3963–9]

Introduction

Hereditary cutaneous malignant melanoma (CMM) is a well-established syndrome (1). One of the main CMM loci has been mapped to chromosome arm 9p21. Three candidate tumor suppressor genes have been identified in this region: *p15/CDKN2B* encodes p15 protein, *p16/CDKN2A* encodes p16 protein, and *p14/ARF* encodes $p14^{ARF}$ protein ($p19^{ARF}$ in mice; ref. 2). $p14^{ARF}$ protein is encoded by an alternative exon 1 (1β) and by exons 2 and 3 of the *p16/CDKN2A* gene in a different reading frame. Consequently, p16 and $p14^{ARF}$ share no homology at the amino acid level and have significantly different functions. p15 and p16 are specific cyclin-dependent kinase (CDK) 4/CDK6 inhibitors in the retinoblastoma (Rb) pathway, and inactivation of p15 and/or p16 allows cells to escape cell cycle arrest in G_1. $p14^{ARF}$ acts in both the p53 and Rb pathways by interacting with MDM2, a protein common to the two pathways. $p14^{ARF}$ binds MDM2 and promotes its degradation, resulting in p53 activation and G_1 and G_2 arrest. *p16/CDKN2A* is currently the most clinically relevant melanoma susceptibility gene in 9p21. By contrast, germ-line mutations in *p14/ARF* are rare (3, 4) and have not been described in *p15/CDKN2B*.

Following the observation that patients with neural system tumors (NST) are at an increased risk of developing CMM, a large population-based survey showed an increased risk of NSTs in melanoma patients and also in their first- and second-degree relatives (5). This has been termed the melanoma-astrocytoma syndrome, owing to the presence of astrocytomas in the first family to be characterized (OMIM 155755; ref. 6). The authors suggested joint predisposition segregating as a Mendelian disorder. Three large deletions have now been reported in families with a hereditary predisposition to melanoma and NSTs: one involving *p15/CDKN2B, p16/CDKN2A*, and *p14/ARF* in a French family (7), one 21,826-pb deletion restricted to exon 1β of *p14/ARF* in a U.S. family (ref. 8, family B in ref. 9), and one probably involving only *p14/ARF* in a U.K. family (ref. 7, family D in ref. 9). Three additional large deletions have been reported in families with a hereditary predisposition to melanoma without NSTs: two involving only *p14/ARF* in a U.S. (10) and in a U.K. family (family A in ref. 9) and one restricted to *p16/CDKN2A* in a U.K. family (family C in ref. 9). It is noteworthy that Mistry et al. (9) suggested coancestry of families A (without NSTs) and B (with NSTs) and concluded that the susceptibility in these two families was primarily to melanoma. Finally, germ-line mutations in *p16/CDKN2* have been reported in families with a hereditary predisposition to melanoma with NSTs (9).

Here, using sequence-tagged site (STS) real-time PCR-based gene dose mapping, we determined the precise size and end points of a large germ-line deletion removing the entire *p15/CDKN2B-p16/CDKN2A-p14/ARF* gene cluster initially detected in a large French melanoma-NST syndrome family (7).

We also identified, within the 403-kb germ-line deletion, a new large antisense noncoding RNA (named *ANRIL*) with a first exon located in the promoter of the *p14/ARF* gene and overlapping the two exons of *p15/CDKN2B*. Expression of this noncoding RNA coclustered mainly with *p14/ARF* in both physiologic and pathologic conditions.

Note: Supplementary data for this article are available at Cancer Research Online (http://cancerres.aacrjournals.org/).

Requests for reprints: Ivan Bièche, Laboratoire de Génétique Moléculaire-Institut National de la Sante et de la Recherche Medicale U745, Faculté des Sciences Pharmaceutiques et Biologiques, Université Paris 5, 4 Avenue de l'Observatoire, 75006 Paris, France. Phone: 33-1-53-73-97-25; Fax: 33-1-44-07-17-54; E-mail: ivan.bieche@univ-paris5.fr.

doi:10.1158/0008-5472.CAN-06-2004

Materials and Methods

Patients. The family with a cluster of CMM and NSTs (Fig. 1) has been investigated since 1977 at Hôpital Pitié-Salpêtrière in Paris, France. About 100 individuals have been surveyed. Pathologic materials initially investigated in 16 different laboratories were, when possible, reassessed by both a dermatopathologist and a neuropathologist. Extensive historical and clinical descriptions of this kindred are available elsewhere (11). Overall, eight members of this family have or had CMM and nine members have or had NSTs, ranging from astrocytoma of all grades to schwannoma, neurofibroma, and meningioma. Six relatives have both skin tumors and NSTs, resulting in statistical cosegregation of the skin tumor and NST traits. This family therefore illustrates a melanoma-NST syndrome probably inherited as a single autosomal dominant Mendelian trait. However, the possibility of other explanations cannot be ruled out for the constellation of tumors observed in this family, such as multiple tightly linked genes or a contiguous gene syndrome.

DNA extraction. High-molecular-weight DNA was prepared by standard proteinase K digestion followed by phenol-chloroform extraction from whole blood leukocytes or lymphoblastoid cell lines from seven individuals, including three affected haplotype-positive relatives (III-16, III-23, and IV-20) and four healthy haplotype-negative relatives (II-9, III-10, III-14, and IV-9). The haplotypes have been defined elsewhere (11).

STS real-time PCR-based gene dose mapping. In this method, quantitative values are obtained from the threshold cycle number at which the increase in the signal associated with exponential growth of PCR products begins to be detected by PE Biosystems analysis software (Perkin-Elmer Applied Biosystems, Foster City, CA), used as recommended in the manufacturer's manuals. The precise amount of genomic DNA added to each reaction mix (based on absorbance) and its quality (i.e., lack of extensive degradation) are both difficult to assess. We therefore also quantified the *ALB* gene (encoding albumin and mapping to chromosome region 4q11-q13) as an endogenous DNA control, and each sample was normalized based on its *ALB* content. The relative STS marker copy number was also normalized to a calibrator, or 1× sample, consisting of genomic DNA from a normal subject.

Final results, expressed as N-fold differences in the target STS marker copy number relative to the *ALB* gene and the calibrator, and termed "N_{STS}," were determined as follows: $N_{STS} = 2^{(\Delta Ctsample - \Delta Ctcalibrator)}$, where ΔCt values of the sample and calibrator are determined by subtracting the average *C*t value of the target STS marker from the average *C*t value of the *ALB* gene. Given the target STS marker, samples with N_{STS} values of 0.5 and 1.0 were considered deleted and normal, respectively. Primers for *ALB* and the 26 9p21-linked STS markers were chosen with the assistance of the computer program Oligo 4.0 (National Biosciences, Plymouth, MN). We conducted BLASTN searches against nr (the nonredundant set of the Genbank, European Molecular Biology Laboratory, and DNA Data Bank of Japan database sequences) to confirm the total STS specificity of the nucleotide sequences chosen for the primers. The primer pairs for each STS were selected to be unique in the human genome; in particular, they were located outside repetitive DNA sequences (Alus, LINEs, etc.). All PCRs were done with an ABI Prism 7700 Sequence Detection System (Perkin-Elmer Applied Biosystems) and the SYBR Green PCR Core Reagents kit (Perkin-Elmer Applied Biosystems). The thermal cycling conditions comprised an initial denaturation step at 95°C for 10 min and 50 cycles at 95°C for 15 s and 65°C for 1 min. Experiments were done with triplicates for each data point.

Fine characterization of the 403-kb germ-line deletion. Long-range PCR was done with the Expand Long Template PCR System (Boehringer Mannheim, Mannheim, Germany) as recommended by the manufacturer. Forward primer STS20 and reverse primer STS17 amplified an ~1.5-kb mutant genomic fragment, the normal fragment being too large (405 kb) to be amplified. PCR products were sequenced with the Applied Biosystems Prism Dye Terminator Cycle Sequencing Ready Reaction kit (Perkin-Elmer Applied Biosystems) and an Applied Biosystems DNA Sequencer Model 310 (Perkin-Elmer Applied Biosystems).

Real-time reverse transcription-PCR. The theoretical and practical aspects of real-time quantitative reverse transcription-PCR (RT-PCR) using the ABI Prism 7700 Sequence Detection System have been described in detail elsewhere (12). Briefly, results, expressed as N-fold differences in target gene (*p15/CDKN2B, p16/CDKN2A, p14/ARF*, or *ANRIL* gene) expression relative to an endogenous RNA control (*PPIA* gene), termed N*target*, are determined by the following formula: N*target* = $2^{\Delta Ctsample}$, where the ΔCt value of the sample is determined by subtracting the *C*t value of the target gene from the *C*t value of the *PPIA* gene. The N*target* values of the samples are subsequently normalized such that the N*target*

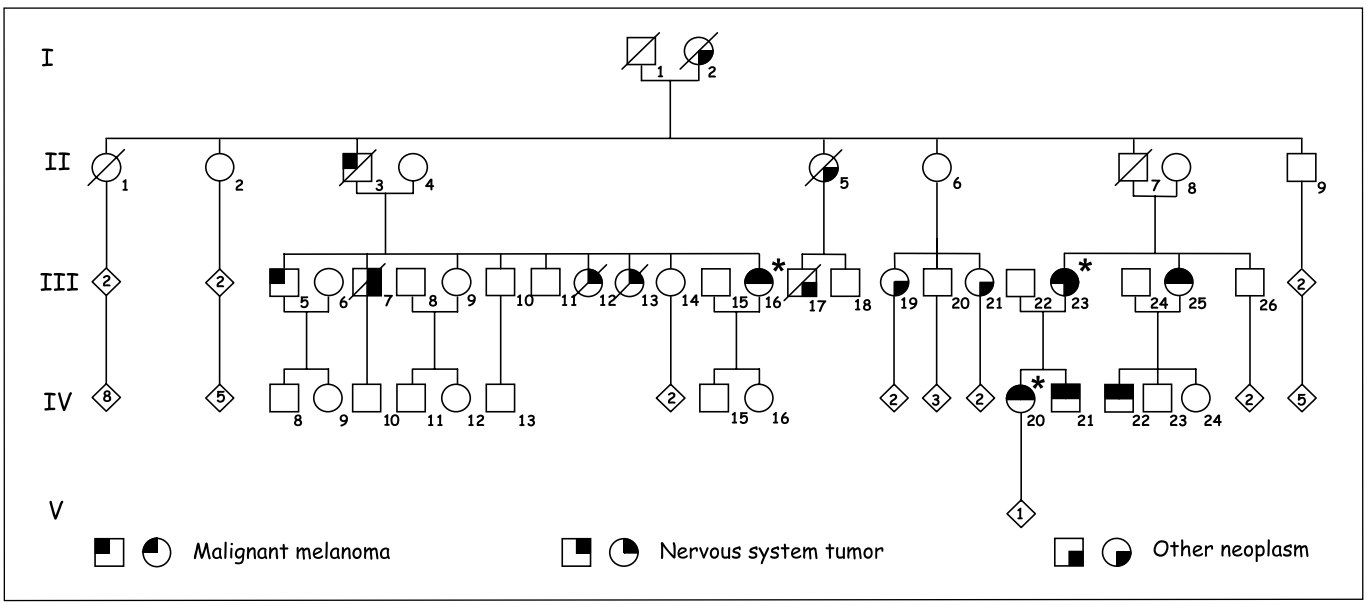

Figure 1. Pedigree of the family with the melanoma-NST syndrome. *Square* and *circle pedigree symbols,* males and females, respectively. *Diamonds,* unaffected siblings of the two sexes. *Number inside the symbol,* multiple individuals. *Asterisks,* the three 403-kb deleted and affected patients tested. Patient III-16 had excision of what proved to be a neurofibroma of the tarsus. An intercostal neurofibroma was excised in patient III-23 at age 32 and a popliteal neurofibroma in her daughter, IV-20, at age 15. The six other NST-affected patients have or had astrocytoma, schwannoma, neurofibroma, or meningioma (11).

Table 1. Oligonucleotide primer sequences used

Genes	Oligonucleotide	Sequence
ANRIL	Upper primer	5′-CAACATCCACCACTGGATCTTAACA-3′
	Lower primer	5′-AGCTTCGTATCCCCAATGAGATACA-3′
p14/ARF	Upper primer	5′-GGTTTTCGTGGTTCACATCCC-3′
	Lower primer	5′-CCCATCATCATGACCTGGTCTT-3′
p16/CDKN2A	Upper primer	5′-CATGGAGCCTTCGGCTGACT-3′
	Lower primer	5′-CCATCATCATGACCTGGATCG-3′
p15/CDKN2B	Upper primer	5′-GAATGCGCGAGGAGAACAAG-3′
	Lower primer	5′-CCATCATCATGACCTGGATCG-3′
PPIA	Upper primer	5′-GTCAACCCCACCGTGTTCTT-3′
	Lower primer	5′-CTGCTGTCTTTGGGACCTTGT-3′

value of the normal human tissue (or of the breast tumor), which contains the smallest amount of target gene mRNA, is 1. The nucleotide sequences of the primers for *PPIA* and for the four target genes are shown in Table 1. To avoid amplification of contaminating genomic DNA, one of the two primers was placed at the junction between two exons. The thermal cycling conditions comprised an initial denaturation step at 95°C for 10 min and 50 cycles at 95°C for 15 s and 65°C for 1 min.

Results and Discussion

In a French family with a history of melanoma and NSTs, we have previously identified a large germ-line deletion, including the entire *p15/CDKN2B-p16/CDKN2A-p14/ARF* gene cluster (7). This family is the largest known melanoma-NST syndrome family, eight members having CMM and nine members having NSTs (six members have both skin tumors and NSTs), ranging from astrocytoma of all grades to schwannoma, neurofibroma, and meningioma (Fig. 1). Microsatellite polymorphism analysis showed heterozygosity at both the centromeric marker D9S976 and the telomeric marker D9S736, suggesting that the deleted region was smaller than 700 kb (Fig. 2). It is noteworthy that a fourth gene, *MTAP*, which encodes methylthioadenosine phosphorylase, is located in this 700-kb region. Behrmann et al. (13) has suggested that MTAP inactivation could be an important step in the development of melanomas.

To determine the precise size and end points of this germ-line deletion, we estimated the number of copies (one or two) by real-time PCR-based gene dosage assay for various STS located between the markers D9S976 and D9S736.

We first analyzed 11 STS markers regularly spaced (every ~70 kb) within the deleted region. Two additional steps, using

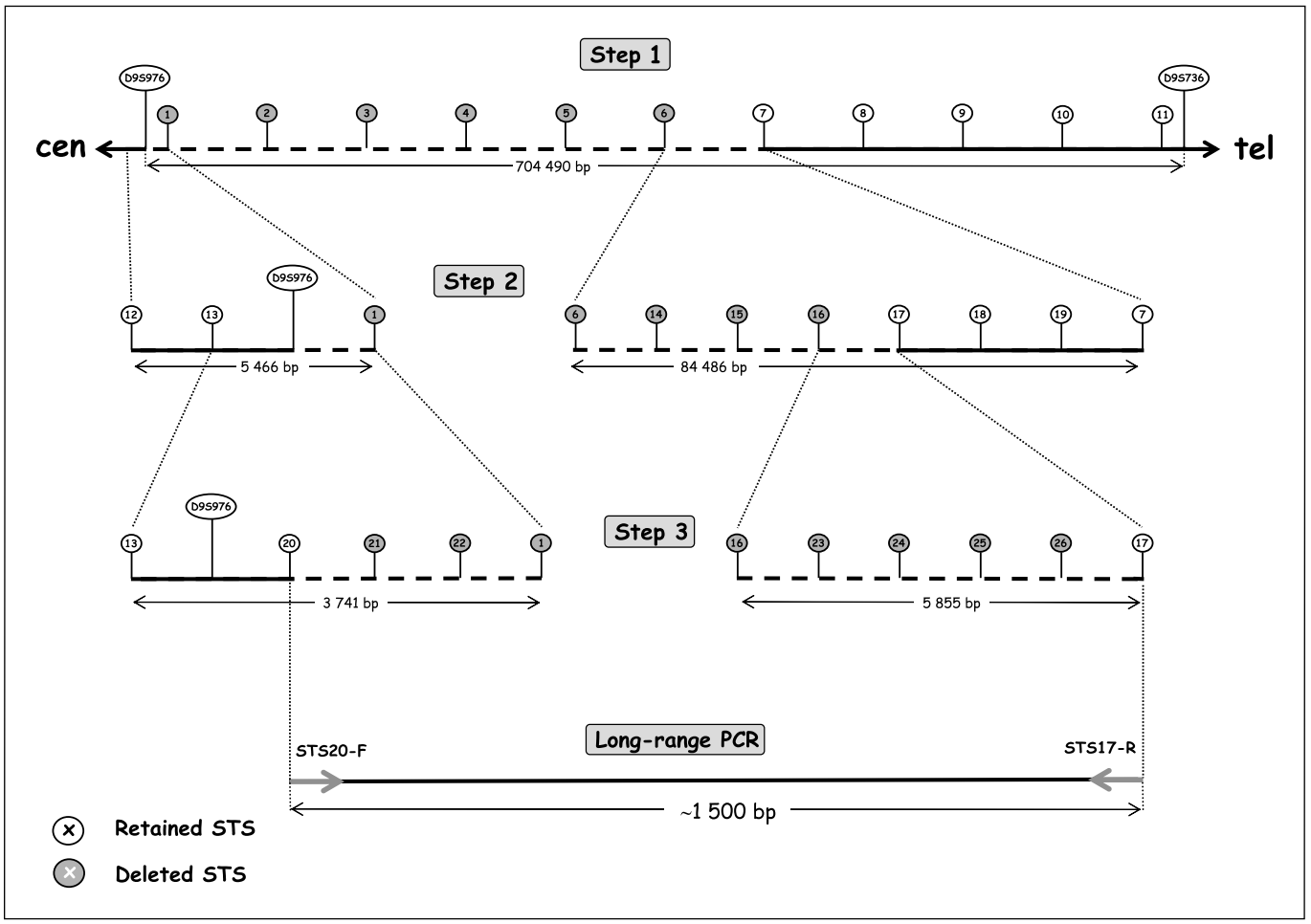

Figure 2. STS real-time PCR-based gene dose mapping assay. Multiple primers were designed to be regularly spaced every ~70 kb (step 1), ~5 kb (step 2), and ~1 kb (step 1) within breakpoint regions. Long-range PCR with the forward primer of the STS20 marker and the reverse primer of the STS17 marker generates a PCR product of ~1.5 kb.

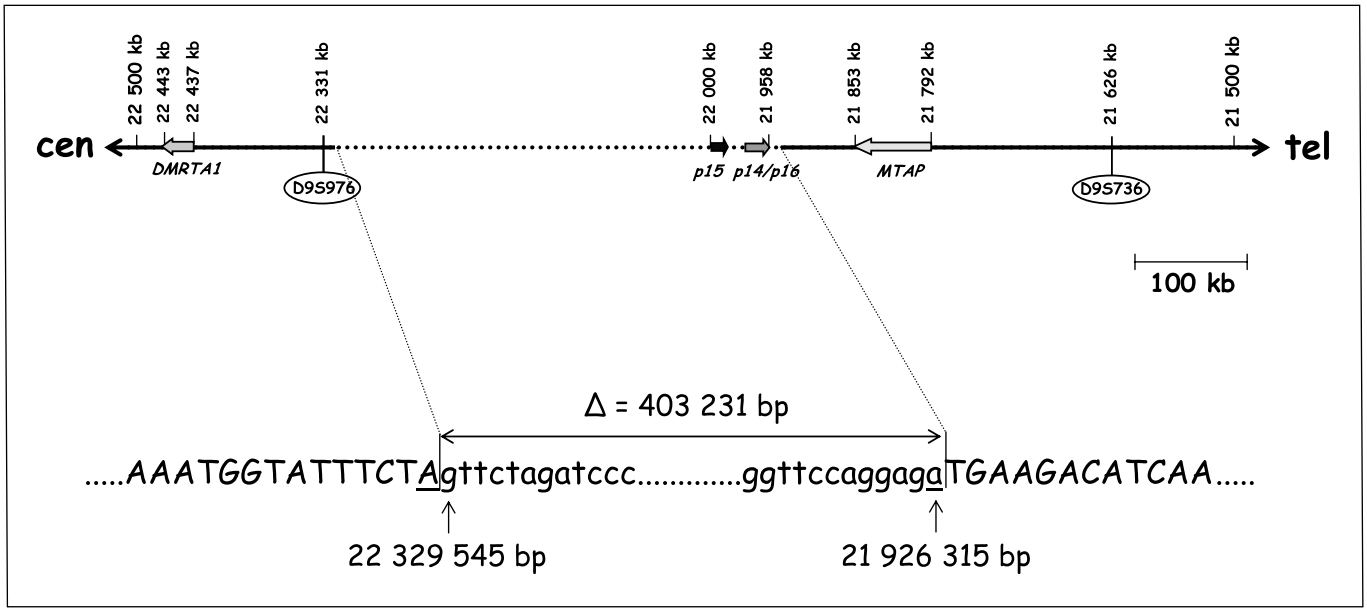

Figure 3. Schematic presentation of the large deletion that includes the entire *p15/CDKN2B-p16/CDKN2A-p14/ARF* gene cluster. *Solid* and *broken horizontal lines,* retained and deleted regions, respectively. *Arrows,* genes. Nucleotide sequences at the deletion end points. *Lowercase letters,* deleted sequences. *Underlined,* a 1-bp repeat sequence (adenine) at the deletion end. *Numbers,* nucleotide positions in the Build 34 NCBI Map Viewer.

carefully chosen additional STS markers (eight and seven markers, respectively), allowed us to refine the centromeric and telomeric breakpoint regions (~1 kb) sufficiently for long-range PCR. The strategy and results are summarized in Fig. 2. Long-range PCR was done on genomic DNA from affected patient by using the forward primer of the retained STS20 marker and the reverse primer of the retained STS17 marker, generating a PCR product of ~1.5 kb. The normal fragment was too large (~405 kb) to be amplified. Sequencing of this PCR product revealed that a sequence between nucleotides 22,329,545 and 21,926,315 [numbered in the Build 34 National Center for Biotechnology Information (NCBI) Map Viewer][4] was deleted in the PCR product (Fig. 3). Thus, the deletion was exactly 403,231 bp long (~403 kb). There were no highly homologous sequences between the two deletion boundaries, and only a 1-bp (adenine) identical sequence at the deletion end points, making it unlikely that the deletion resulted from an unequal homologous recombination event. It is noteworthy, however, that the centromeric breakpoint is located within a truncated LINE element.

The 403-kb germ-line deletion included the entire *p15/CDKN2B-p16/CDKN2A-p14/ARF* gene cluster but unambiguously excluded additional well-characterized genes, namely *MTAP* (NM_002451) located in the telomeric region and *DMRTA1* (NM_022160) in the centromeric region (Fig. 3).

To develop a direct predictive test for this large French family with the melanoma-NST syndrome associated with a 403-kb germ-line deletion, additional primers (Δ403-U: 5′-CCAGTCTATCGTTGTTGGACAT-3′ and Δ403-L: 5′-TGTATTTGATGGCATTCCACA-3′) were designed to obtain a short PCR product (210 bp) in a simple and rapid assay designed to detect the junction fragment. Our results indicate that PCR-based detection of the junction fragment is an effective and direct method for the identification of subjects with an individual risk in this family (Fig. 4). Indeed, the three affected individuals tested yielded the 210-bp fragment, whereas the four healthy relatives tested did not.

A search of the dbEST database, using the Gapped BLAST program (14), allowed us to identify several human expressed sequence tags (EST) of an unidentified transcript (Genbank accession nos. CN277071, AA807394, BF002332, BI765545, BX100299, AI825844, AW169296, and BC038540). Some of these ESTs contained a polyadenylation site, suggesting that this gene is transcribed in the direction opposite from the *p15/CDKN2B-p16/CDKN2A-p14/ARF* gene cluster. RT-PCR amplification of a cDNA obtained from normal human testis mRNA, using various primers placed in the identified ESTs, and sequence analysis of the PCR products, identified a large cDNA 3,834 bp long. This cDNA seems to be untranslated, as it does not possess a clear open reading frame. We chose to name this novel gene *ANRIL*, for "antisense noncoding RNA in the *INK4* locus" (Genbank accession no. DQ485453). Alignment of the *ANRIL* 3,834-bp cDNA with genomic sequence led to the conclusion that the *ANRIL* gene contains 19 exons, with exon/intron junctions corresponding to the consensus sequences of donor/acceptor splice sites and a polyadenylation site in the last exon. The *ANRIL* genomic sequence spans a region of 126.3 kb. We also characterized a short alternatively spliced *ANRIL* mRNA species 2,659 bp long, composed of the first 12 *ANRIL* exons and an additional 3′ exon (located in intron 12), including a second polyadenylation site (Genbank accession no. DQ485454).

The *ANRIL* gene overlaps the two exons of *p15/CDKN2B* but does not share any nucleotide sequences (Fig. 5*A*). Moreover, the 5′ end of the first exon of the *ANRIL* gene is located about −300 bp upstream of the transcription start site of the *p14/ARF* gene, suggesting that these two genes may share a bidirectional promoter (Fig. 5*A*). Global transcriptome analysis recently provided evidence that the bulk of the mammalian genome can produce transcripts from both stands, with a large number of novel noncoding RNAs

[4] http://genome.ucsc.edu/cgi-bin/hgTracks?position=chr9

(15). The latter authors also showed the existence of a large number of transcription units (paired sense/antisense transcripts) in the mammalian genome and suggested that antisense transcription contributes to controlling transcriptional outputs (16). For example, these authors identified 1,092 coding-noncoding pairs overlapping head to head on the promoter in the mouse genome.

To test the possible coordinated transcriptional regulation of *ANRIL* and *p14/ARF*, we quantified *ANRIL, p14/ARF, p16/CDKN2A*, and *p15/CDKN2B* mRNA in 22 normal human tissues (Supplementary Fig. S1*A*). The highest expression of *ANRIL* was observed in normal ovary, and the lowest expression was observed in skeletal muscle (100-fold lower than in ovary). *ANRIL* coclustered with *p14/ARF, p16/CDKN2A*, and *p15/CDKN2B* in these normal human tissues, with a stronger positive correlation between *ANRIL* and *p14/ARF* (Spearman rank correlation test: $r = +0.949$; $P < 10^{-7}$) than between *ANRIL* and *p16/CDKN2A* ($r = +0.573$; $P = 0.004$) or between *ANRIL* and *p15/CDKN2B* ($r = +0.561$; $P = 0.005$). In a series of 12 breast tumor tissues showing a wide range of *p14/ARF, p16/CDKN2A*, and *p15/CDKN2B* mRNA levels, we also observed a stronger positive correlation of *ANRIL* with *p14/ARF* (Spearman rank correlation test: $r = +0.965$; $P = 0.000001$) than with *p16/CDKN2A* ($r = +0.902$; $P = 0.00008$) or *p15/CDKN2B* ($r = +0.769$; $P = 0.004$; Supplementary Fig. S1*B*). Finally, in an additional series of NF1-associated tumors in tissues derived from the embryonic neural crest (the Schwann cells are considered to be the progenitors of these tumors), we confirmed the positive link between the expression of *ANRIL* with *p14/ARF* as well as with *p16/CDKN2A* and *p15/CDKN2B* (data not shown) in a second tumor type.

These data suggest coordinated transcriptional regulation of *ANRIL* and *p14/ARF*, and possibly also *p16/CDKN2A* and *p15/CDKN2B*, in both physiologic and pathologic conditions.

At the moment, it is difficult to propose a mechanism of action for noncoding RNA. Indeed, the puzzle of noncoding RNA in eukaryotes is just starting to be assembled, and certainly, further unexpected pieces will be identified in the near future. To date, it likely seems that noncoding RNAs constitute a critical hidden layer of gene regulation in complex organisms, and their understanding requires new approaches in functional assays (17). We can hypothesize that *ANRIL* (antisense gene) could regulate *p15/CDKN2B-p16/CDKN2A-p14/ARF* locus (sense genes) by various novel mechanisms, such as RNA interference, gene cosuppression, gene silencing, chromatin structure maintenance, imprinting, and DNA demethylation (18). Moreover, we cannot rule out the possibility that *ANRIL* gene could be able to produce mature miRNAs (19) or encode a small peptide (20). Additional studies are thus necessary to elucidate the putative role via a genetic (or epigenetic) mechanism of *ANRIL* gene on the regulation (deregulation in tumorigenesis) of the *p15/CDKN2B-p16/CDKN2A-p14/ARF* locus.

Further studies of *ANRIL* and/or *p14/ARF* and/or *p15/CDKN2B* will be necessary to explain the additional tumor spectrum (i.e., NSTs) in this French family. Indeed, *p15/CDKN2B* and *p14/ARF*, like *p16/CDKN2A*, are altered during NST progression (21–23), but no germ-line mutation of *p15/CDKN2B* or *p14/ARF* has been clearly implicated in inherited predisposition to NSTs (24). With regard to the *ANRIL* gene, we reanalyzed (Fig. 5*B*) the large 9p21 germ-line deletions previously reported in families with a hereditary predisposition to melanoma with or without NSTs (7–10). *ANRIL* was entirely deleted in our French family with NSTs (family F in Fig. 5*B*). *ANRIL* exon 1 was deleted in two U.K. families, one with and one without NSTs (families B and A, respectively), whereas its promoter was unambiguously deleted in one U.S. family without NSTs (families E) and probably deleted in another U.S. family with NSTs (families D). However, it could be hypothesized that these

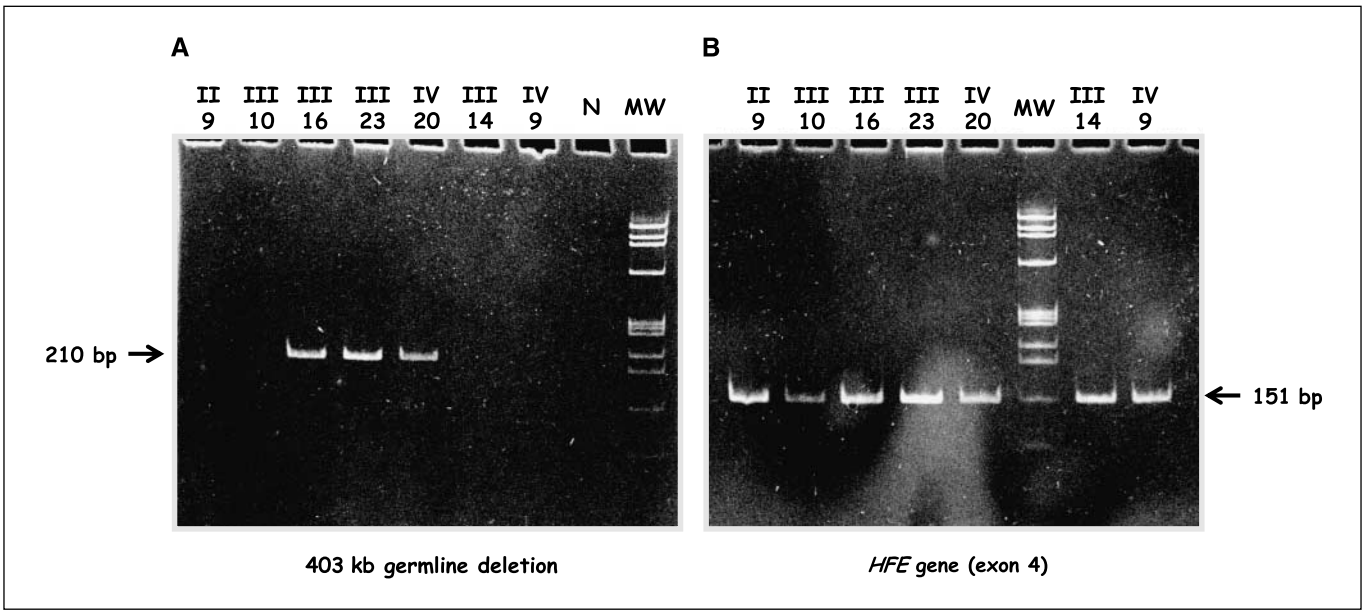

Figure 4. *A,* PCR detection of the 403-kb germ-line deletion. Only the affected relatives (III-16, III-23, and IV-20) yielded a 210-bp fragment (*arrow*) with the primers Δ403-U (5′-CCAGTCTATCGTTGTTGGACAT-3′) and Δ403-L (5′-TGTATTTGATGGCATTCCACA-3′), whereas the healthy relatives (II-9, III-10, III-14, and IV-9) yielded no PCR product, the wild-type allele being too large (403,441 bp) to be amplified. *N,* high-quality normal human genomic DNA. *MW,* molecular weight marker. *B,* PCR control of the amount of genomic DNA added to each reaction. Genomic DNAs were amplified with a primer pair located in exon 4 of the *HFE* gene (NM_000410), generating a 151-bp fragment (*arrow*) in all patients tested.

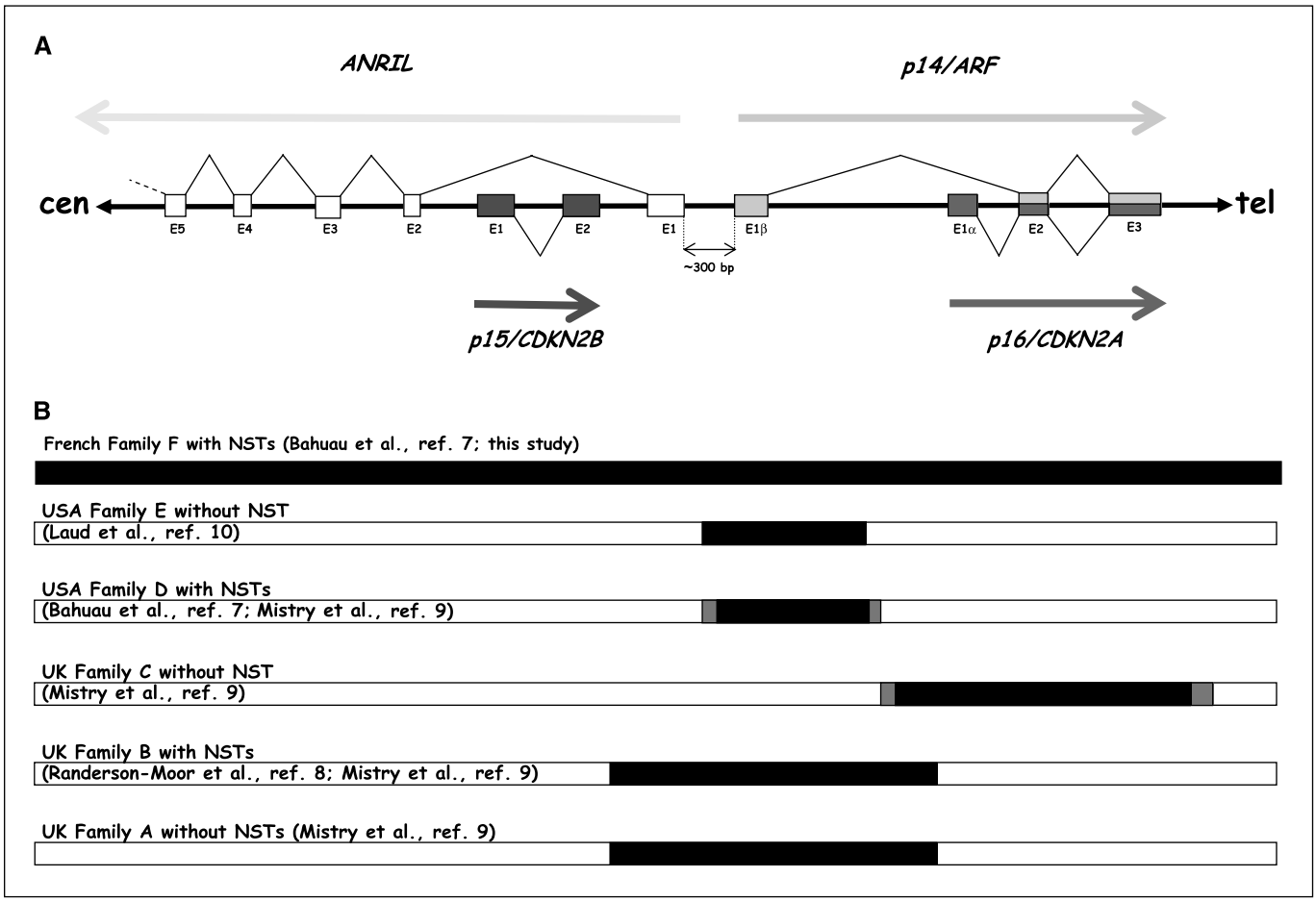

Figure 5. *A,* genomic organization of the *p15/CDKN2B-p16/CDKN2A-p14/ARF* gene cluster. *Boxes,* location of exons (approximately to scale). Exons 1α, 2, and 3 of *p16/CDKN2A* encode p16 protein, whereas exon 1β, spliced to exons 2 and 3 of *p16/CDKN2A* in a different reading frame and transcribed using a different promoter, encodes $p14^{ARF}$ protein. The *ANRIL* gene overlaps the two exons of *p15/CDKN2B* and is transcribed in the orientation opposite to the *p15/CDKN2B-p16/CDKN2A-p14/ARF* gene cluster. Exon 1 of *ANRIL* is present about −300 bp upstream of the transcription start site of *p14/ARF* (exon 1β). *B,* compiled literature on physical and family deletion maps of the *p15/CDKN2B-p16/CDKN2A-p14/ARF* gene cluster region. *Black rectangles,* deleted regions in families A, B, C, D, E, and F. *Gray parts of the rectangles,* in families C and D, the limits of the candidate regions of the breakpoints.

two U.S. families D and E, like the two U.K. families A and B (see ref. 9), could have an identical deletion of coancestral origin. Finally, the *ANRIL* gene was not deleted in a second U.K. family without NSTs (family C). Location of deletion end points of each large deletion reported in these different families needs to be fully characterized to further incriminate *ANRIL* as a putative candidate gene in melanoma-NST syndrome susceptibility.

The identification of this large antisense noncoding RNA could be important in cancer pathology as in hereditary predisposition to melanoma or in somatic alteration of the *p15/CDKN2B-p16/CDKN2A-p14/ARF* cluster observed in a large proportion of cancers, but also important in physiology area, the *p15/CDKN2B-p16/CDKN2A-p14/ARF* locus having a key role in the replicative senescence. Recent studies suggest that alteration of an antisense RNA can alter the expression of the corresponding sense mRNAs (25). Alteration of this noncoding RNA could be obtained by large deletion (including the entire *ANRIL* gene as in our family), deletion of one or several exons, deletion of a part of the promoter, splice sites mutations, aberrant DNA methylation (only in the somatic tumor), etc.

In conclusion, by applying STS real-time PCR-based gene dose mapping to a French melanoma-NST syndrome family, we identified a germ-line deletion encompassing a new putative transcriptional regulator gene (i.e., *ANRIL*) and the entire *p15/CDKN2B-p16/CDKN2A-p14/ARF* gene cluster. Our data suggest coordinated transcriptional regulation of *ANRIL* and *p14/ARF* (and, to a lesser extent, *p16/CDKN2A* and *p15/CDKN2B*) in both physiologic and pathologic conditions. Further studies are necessary to elucidate the role of the *ANRIL* gene in melanoma-NST syndrome families, in melanoma-prone families with no identified *p16/CDKN2A* mutations, and in somatic tumors.

Our new simple and rapid gene dose mapping assay should prove useful for characterizing other large germ-line deletions in research settings.

Acknowledgments

Received 6/1/2006; revised 11/17/2006; accepted 2/9/2007.

Grant support: Association pour la Recherche sur le Cancer and Ministère de l'Enseignement Supérieur et de la Recherche.

The costs of publication of this article were defrayed in part by the payment of page charges. This article must therefore be hereby marked *advertisement* in accordance with 18 U.S.C. Section 1734 solely to indicate this fact.

References

1. Hayward NK. Genetics of melanoma predisposition. Oncogene 2003;22:3053–62.
2. Lowe SW, Sherr CJ. Tumor suppression by Ink4a-Arf: progress and puzzles. Curr Opin Genet Dev 2003;13:77–83.
3. Rizos H, Darmanian AP, Holland EA, Mann GJ, Kefford RF. Mutations in the INK4a/ARF melanoma susceptibility locus functionally impair p14ARF. J Biol Chem 2001;276:41424–34.
4. Hewitt C, Lee Wu C, Evans G, et al. Germline mutation of ARF in a melanoma kindred. Hum Mol Genet 2002;11:1273–9.
5. Azizi E, Friedman J, Pavlotsky F, et al. Familial cutaneous malignant melanoma and tumors of the nervous system. A hereditary cancer syndrome. Cancer 1995;76:1571–8.
6. Kaufman DK, Kimmel DW, Parisi JE, Michels VV. A familial syndrome with cutaneous malignant melanoma and cerebral astrocytoma. Neurology 1993;43:1728–31.
7. Bahuau M, Vidaud D, Jenkins RB, et al. Germ-line deletion involving the INK4 locus in familial proneness to melanoma and nervous system tumors. Cancer Res 1998;58:2298–303.
8. Randerson-Moor JA, Harland M, Williams S, et al. A germline deletion of p14(ARF) but not CDKN2A in a melanoma-neural system tumour syndrome family. Hum Mol Genet 2001;10:55–62.
9. Mistry SH, Taylor C, Randerson-Moor JA, et al. Prevalence of 9p21 deletions in UK melanoma families. Genes Chromosomes Cancer 2005;44:292–300.
10. Laud K, Marian C, Avril MF, et al. Comprehensive analysis of CDKN2A (p16INK4A/p14ARF) and CDKN2B genes in 53 melanoma index cases considered to be at heightened risk of melanoma. J Med Genet 2006;43:39–47.
11. Bahuau M, Vidaud D, Kujas M, et al. Familial aggregation of malignant melanoma/dysplastic naevi and tumours of the nervous system: an original syndrome of tumour proneness. Familial aggregation of malignant melanoma/dysplastic naevi and tumours of the nervous system: an original syndrome of tumour proneness. Ann Genet 1997;40:78–91.
12. Bieche I, Parfait B, Le Doussal V, et al. Identification of CGA as a novel estrogen receptor-responsive gene in breast cancer: an outstanding candidate marker to predict the response to endocrine therapy. Cancer Res 2001;61:1652–8.
13. Behrmann I, Wallner S, Komyod W, et al. Characterization of methylthioadenosin phosphorylase (MTAP) expression in malignant melanoma. Am J Pathol 2003;163:683–90.
14. Altschul SF, Madden TL, Schäffer AA, et al. Gapped BLAST and PSI-BLAST: a new generation of protein database search programs. Nucleic Acids Res 1997;25:3389–402.
15. Carninci P, Kasukawa T, Katayama S, et al. The transcriptional landscape of the mammalian genome. Science 2005;309:1559–63.
16. Katayama S, Tomaru Y, Kasukawa T, et al. Antisense transcription in the mammalian transcriptome. Science 2005;309:1564–6.
17. Mattick JS. The functional genomics of noncoding RNA. Science 2005;239:1527–8.
18. Costa F. Non-coding RNAs: new players in eukaryotic biology. Gene 2005;357:83–94.
19. Calin GA, Croce CM. MicroRNA-cancer connection: the beginning of a new tale. Cancer Res 2006;64:7390–4.
20. Chooniedass-Kothari S, Emberley E, Hamedani MK, et al. The steroid receptor RNA activator is the first functional RNA encoding a protein. FEBS Lett 2004;566:43–7.
21. Jen J, Harper JW, Bigner SH, et al. Deletion of p16 and p15 genes in brain tumors. Cancer Res 1994;54:6353–8.
22. Izumoto S, Arita N, Ohnishi T, Hiraga S, Taki T, Hayakawa T. Homozygous deletions of p16INK4A/MTS1 and p15INK4B/MTS2 genes in glioma cells and primary glioma tissues. Cancer Lett 1995;97:241–7.
23. Bostrom J, Meyer-Puttlitz B, Wolter M, et al. Alterations of the tumor suppressor genes CDKN2A (p16(INK4a)), p14(ARF), CDKN2B (p15(INK4b)), and CDKN2C (p18(INK4c)) in atypical and anaplastic meningiomas. Am J Pathol 2001;159:661–9.
24. Gao L, Liu L, van Meyel D, et al. Lack of germline mutations of CDK4, p16(INK4A), and p15(INK4B) in families with glioma. Clin Cancer Res 1997;3:977–81.
25. Wahlestedt C. Natural antisense and noncoding RNA transcripts as potential drug targets. Drug Discov Today 2006;11:503–8.

Characterization of a Germ-Line Deletion, Including the Entire *INK4/ARF* Locus, in a Melanoma-Neural System Tumor Family: Identification of *ANRIL*, an Antisense Noncoding RNA Whose Expression Coclusters with *ARF*

Eric Pasmant, Ingrid Laurendeau, Delphine Héron, et al.

Cancer Res 2007;67:3963-3969.